Opto-Mechanical Fiber Sensing of Gamma Radiation

Yosef London, Kavita Sharma, Hilel Hagai Diamandi, Mirit Hen, Gil Bashan, Elad Zehavi, Shlomi Zilberman,
Garry Berkovic [ORCID], Amnon Zentner, Moshe Mayoni, Andrei Aleksandrovich Stolov [ORCID], Mikhail Kalina,
Olga Kleinerman, Ehud Shafir [ORCID], and Avi Zadok [ORCID]

Abstract—The monitoring of ionizing radiation is critical for the safe operation of nuclear and other high-power plants. Fiber-optic sensing of radiation has been pursued for over 45 years. Most protocols rely on radiation effects on the optical properties of the fiber. Here we propose a new concept, in which the opto-mechanics of standard fibers coated by thin layers of fluoroacrylate polymer are observed instead. The time-of-flight of radial acoustic waves through the coating is evaluated by forward stimulated Brillouin scattering measurements. The time-of-flight is seen to decrease monotonically with the overall dosage of gamma radiation from a cobalt source. Variations reach 15% of the initial value for 180 Mrad dose and remain stable for at least several weeks following exposure. The faster times-of-flight are consistent with a radiation-induced increase in the coating stiffness, observed in offline analysis. The effects on the coating are independent of possible changes in the optical parameters of the fiber. The combination of opto-mechanical analysis together with established fiber sensing protocols may help disambiguate the evaluation of multiple radiation metrics and reduce environmental cross-sensitivities. The technique is suitable for online monitoring and may be extended to spatially distributed measurements.

Index Terms—Coatings, nonlinear fiber-optics, optical fiber sensors, opto-mechanics, radiation monitoring, stimulated Brillouin scattering.

I. INTRODUCTION

THE monitoring of ionizing radiation is essential for the proper and safe operation of nuclear and other high-energy

Yosef London, Shlomi Zilberman, Garry Berkovic, and Ehud Shafir are with the Applied Physics Division, Soreq NRC, Yavne 81800, Israel (e-mail: yoseflondon@gmail.com; shlomiz@soreq.gov.il; garry@soreq.gov.il; shafir@soreq.gov.il).

Kavita Sharma, Hilel Hagai Diamandi, Mirit Hen, Gil Bashan, Elad Zehavi, and Avi Zadok are with the Faculty of Engineering and the Institute for Nano-Technology and Advanced Materials, Bar-Ilan University, Ramat-Gan 5290002, Israel (e-mail: kavita1501sharma@gmail.com; hagaid@gmail.com; mirithen071110@gmail.com; gillbashan@gmail.com; eladza93@gmail.com; avinoam.zadok@biu.ac.il).

Amnon Zentner and Moshe Mayoni are with the Technologies Division, Soreq NRC, Yavne 81800, Israel (e-mail: amnon-44@inter.net.il; moshema@soreq.gov.il).

Andrei Aleksandrovich Stolov is with OFS, Avon, CT 06001 USA (e-mail: stolov@ofsoptics.com).

Mikhail Kalina and Olga Kleinerman are with the Department of Materials Science and Engineering, Technion - Israel Institute of Technology, Haifa 32000, Israel (e-mail: mkalina@technion.ac.il; olgakl@technion.ac.il).

Color versions of one or more figures in this article are available at https://doi.org/10.1109/JLT.2021.3102698.

Digital Object Identifier 10.1109/JLT.2021.3102698

plants, waste disposal sites and research facilities. Measurement capabilities become critical in cases of catastrophic failure, such as the Fukushima incident of 2011 [1]. Most radiation dosimeters are restricted to point-sensing [2], [3], which is difficult to scale for the coverage of large areas. Point sensors also require electrical or wireless connectivity and the supply of energy to each measurement location [2], [3], which may fail in case of an accident. Standard optical fibers constitute an exceptional sensing platform [4], [5]. They enable measurements from long stand-off distances, are easily embedded within many structures, comparatively immune to electromagnetic interference, suitable for harsh and hazardous environments, and may continue to operate even where electrical shutdown had occurred. Moreover, optical fibers support spatially distributed analysis, in which every section becomes an independent node in a passive sensor network [6]–[8].

The effects of ionizing radiation on optical fibers have been studied for over 45 years [9], and they are investigated over fibers installed in several large-scale facilities [10]–[12]. The results provide the basis for optical fiber sensors of ionizing radiation [10], [11], [13]–[21]. Most sensors monitor the effects of radiation on optical properties of the fiber, such as induced attenuation or refractive index variations [13]–[29]. For example, attenuation in a standard single-mode fiber at 1,550 nm wavelength increased to $42 \, \text{dB} \times \text{km}^{-1}$ following exposure to 7.3 Mrad of gamma radiation from a ^{60}Co source [24]. Despite much effort and progress, fiber-optic sensors of ionizing radiation still face several challenges. Attenuation and index changes depend on multiple metrics such as radiation type, energy, overall dose, and rate [13]–[29], thus the unambiguous interpretation of results can become difficult. In addition, radiation effects may be influenced by the presence and concentration of trace dopants in the fibers, and by the history of previous exposures and recovery [13]–[29]. Radiation effects on optical fibers are also characterized by cross-sensitivities to other environmental conditions such as temperature [30]–[32].

Fewer works addressed the effects of radiation on mechanical properties of optical fibers. Several studies monitored radiation induced changes to the backward Brillouin scattering frequency shift [33]–[35], which depends on both the refractive index and the velocity of dilatational acoustic waves in the core of the fiber [7], [8]. In another example, changes in the density of silica were observed following exposure to neutron radiation [36]. The fibers may also suffer radiation-induced damage via their coating layers. In one study, the tensile strengths of fibers coated by an ethylene tetrafluoroethylene polymer buffer layer were degraded

following gamma irradiation [37], [38]. The strength reduction was attributed to the release of hydrogen fluoride from the buffer layer, which corroded and weakened the silica fiber [37], [38].

Radiation can also affect coating layers outside optical fibers. A series of studies by Rizzolo and coworkers has shown that both temperature and radiation exposure could modify the elastic properties of several types of coating, or the interface between fiber and coating [39]–[42]. These changes are manifested in distributed temperature measurements through optical frequency domain reflectometry (OFDR), and may alter their proper calibration [39]–[42]. Pre-treatments of temperature cycles or radiation exposure were proposed and established to reduce such inaccuracies [39]–[42]. Possible weakening of the coatings themselves was investigated as well [43]. However, the monitoring of fiber coating properties towards radiation detection and sensing was not considered to-date.

Starting in 2016, a new concept for optical fiber sensing has been proposed and demonstrated, based on fiber opto-mechanics [44]. Short and intense optical pump pulses stimulate a wave packet of guided acoustic modes, which propagate outward in the radial direction from the core of the fiber towards the cladding edge [45]. Multiple reflections take place at the cladding outer boundary. Their magnitudes depend on the elastic properties of the surrounding medium [44]. Echoes of the acoustic wave packet across the fiber core are monitored through photo-elastic phase modulation of an optical probe. The measurements were shown to provide quantitative analysis of liquids outside the cladding of standard, unmodified fiber, where light cannot reach [44]. The principle was successfully extended to spatially distributed analysis, with resolution recently reaching meter-scale [46]–[49]. The acoustic wave packet may also propagate through certain thin layers of coating outside the fiber cladding [50]–[52]. Multiple acoustic reflections then take place, at the boundaries between cladding and coating and between coating and air. The timing of reflections directly indicates the acoustic time-of-flight across the coating and can identify changes in metrics such as thickness, density and stiffness [52].

In this work, we report the effect of ionizing radiation on the opto-mechanics of standard single-mode fiber coated by a thin layer of fluoroacrylate polymer. The acoustic time-of-flight across the coating monotonically decreases with the overall dosage of constant-rate gamma radiation from a ^{60}Co source. Changes remain stable for at least several weeks following exposure. The faster times-of-flight are consistent with an increase in the coating layer stiffness following irradiation, observed using offline pico-indenter measurements [53], [54]. The results provide first proof for a new potential concept of fiber-optic radiation detection and monitoring, based on the elastic characteristics of the coating layer rather than the optical properties of the fiber itself. The technique can complement established fiber-optic sensing protocols, such as measurements of radiation-induced attenuation, index changes or Brillouin shift modifications. The introduction of additional and independent observables may help disambiguate the analysis of multiple radiation metrics and remove cross-sensitivities to environmental conditions. The method is suitable for continuous monitoring

of fibers within protective cables, and it is scalable to spatially distributed analysis.

II. PRINCIPLE OF OPERATION AND RESULTS

A. Principle of Operation

The principles of opto-mechanical fiber sensing based on forward Brillouin scattering are presented in detail in several recent references [44], [46]–[50]. A brief description is reiterated below. Standard optical fibers support a discrete set of radially symmetric acoustic modes that are guided by their entire cross-sections and propagate in the axial direction [45]. Each mode is characterized by a cut-off frequency, below which it may not propagate. The cut-off frequencies of relevant modes are in the range of few hundreds of MHz. The guided acoustic modes may be stimulated by beating among the constituent spectral components of nanosecond-duration, intense optical pump pulses [44]–[52]. Optical stimulation is wavenumber-matched only very close to the cut-off frequencies of the acoustic modes [45]. At that limit the axial wavenumber of the acoustic modes, while not strictly zero, is very small and the wave vectors become almost entirely transverse. The material displacement vectors are predominantly confined to the transverse plane as well. Pump pulses therefore launch a wave packet of multiple transverse, guided acoustic modes, in each cross-section of the fiber. The optically stimulated wave packet propagates outward in the radial direction, from the core of the fiber towards the outer edge of the cladding.

Consider fibers that are coated by a thin polymer layer and kept in air. The acoustic wave packet undergoes multiple partial reflections at the interface between the silica cladding and the polymer coating and at the outer boundary of the coating. The reflectivity values depend on the mechanical impedance of the coating layer [50]–[52]. Reflections form a series of delayed echoes of the acoustic wave packet across the core of the fiber. The acoustic echoes eventually decay on time scales between tens of nanoseconds and few microseconds due to dissipation in silica and coating. The series of acoustic echoes may be monitored through photo-elastic phase modulation of a continuous probe wave that co-propagates with the pump pulses [44]. The modulation of the optical probe is wavenumber matched with the optically stimulated acoustic modes over a broad range of wavelengths [45].

We assume that the cross-sections of fibers under test are uniform and that external conditions do not vary along their axes. In these cases, the photo-elastic phase modulation of the probe accumulates over the length of the fiber, and its instantaneous magnitude at the output is proportional to that of the acoustic wave packet across the core in every cross-section [45]. The temporal dynamics of acoustic perturbations can become rather complex [50]–[52]. Nevertheless, the time difference between specific events may be related to the two-way time-of-flight of dilatational acoustic waves across the coating layer ([52], see also below). In a previous study, pump-probe opto-mechanical measurements were used to characterize the temperature dependence of the acoustic velocity in several types of coatings
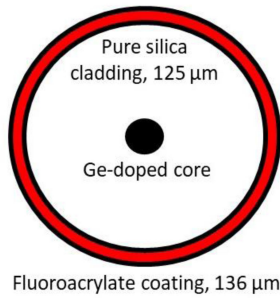
Fig. 1. Schematic cross-section of the single-mode fiber used in experiments.
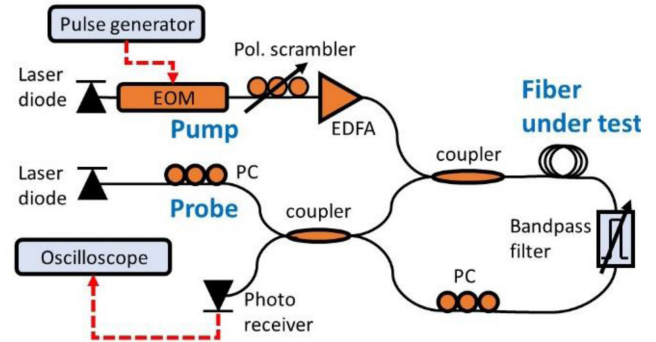

Fig. 2. Schematic illustration of the measurement setup of fiber opto-mechanics [52]. PC: polarization controller; EOM: electro-optic Mach-Zehnder intensity modulator; EDFA: erbium-doped fiber amplifier.

[52]. In this work, we observe the effects of gamma radiation on the acoustic time-of-flight through a specific thin coating layer.

The coating layer must be comparatively thin and with low acoustic losses, or else the acoustic wave packet might not reach its outer boundary. For example, standard dual-layer or single-layer acrylate coatings strongly absorb the acoustic waves, and do not support measurements of two-way acoustic times-of-flight. Polyimide coating layers exhibit sufficiently low acoustic dissipation [50], [51]. However, we did not observe measurable changes in the acoustic time-of-flight through polyimide coatings following exposure to gamma radiation from a cobalt source, up to an overall dose of 110 Mrad (see below).

Fluoroacrylate coating of single-mode fibers is commercially available and has low enough acoustic dissipation to allow for times-of-flight measurements. The coating is designed for a low index of 1.405 refractive index units. Due to inherently low refractive indices, fluoroacrylate coatings also serve as light guiding claddings in different specialty optical fibers [55]. Unlike polyimide, the acoustic times-of-flight through the fluoroacrylate layer did change with exposure to gamma radiation, as described in detail next. We therefore chose this type of coating for quantitative experiments. The coating outer diameter was 136 μm, chosen based on availability.

The single-mode fiber under test was provided by OFS company. It was drawn from an SMF-28-compatible, G.652 preform, and had a germanium-doped silica core and a pure silica cladding of 125 μm diameter. The specifications of the core have little effect on measurements of acoustic times-of-flight through the coating. The fiber was coated by fluoroacrylate polymer at production. The fiber cross-section is illustrated in Fig. 1.

B. Experimental Results

Eleven sections under test, each between 6–10 meters long, were taken from a continuous, 100 meters-long reel of the above fiber. Each section was exposed to gamma radiation of 1.173 MeV and 1.332 MeV energies from a ^{60}Co source (FTS 812 Foss Therapy Services Inc.), at a fixed nominal rate of 2.4 Mrad per day, for a different duration of 1–10.5 weeks (accumulated dosages of 17–180 Mrad). The uncertainty of all dosages is $\pm 5\%$. Temperature during irradiation varied between 20–30 °C. The opto-mechanical measurements of each fiber sample were carried out in a different laboratory, after its irradiation period had ended. Opto-mechanical pump-probe traces of each sample

were taken the day after the end of its exposure, and four more times over the course of few weeks.

The opto-mechanical measurement setup is illustrated in Fig. 2 (for greater detail see [44], [56].) The section of fiber under test was placed within a Sagnac interferometer loop [56]. Light from a first laser diode at 1,550 nm wavelength was intensity modulated to obtain pump pulses of 1.5 ns duration and 5 μs period. The pump pulses were amplified by an erbium-doped fiber amplifier to 300 mW average power and launched into the section under test in the clockwise direction only. Each pump pulse stimulated a wave packet of radial guided acoustic modes as described above. A polarization scrambler on the pump path was used to suppress the contributions of non-radial guided acoustic modes [44], [45], [56]. A tunable optical bandpass filter blocked the pump pulses from reaching the loop output.

Continuous wave light of 1,532 nm wavelength and 30 mW power from a second laser diode served as an optical probe and was coupled into the loop in both directions. The clockwise propagating probe wave replica underwent photo-elastic phase modulation in the fiber section under test due to the stimulated acoustic waves. The counterclockwise propagating probe acquired much weaker phase modulation due to the lack of wavenumber matching [44], [45], [56]. The beating of the two probe wave components at the loop output converted the non-reciprocal photo-elastic phase modulation into an intensity signal. Polarization controllers were adjusted to obtain maximum intensity variations at the loop output [44]. The output probe wave was detected by a photo-receiver of 27 V $\times$ W^{-1} responsivity and 15 ps rise time. The instantaneous receiver voltage was proportional to the magnitude of the acoustic wave packet across the core in each fiber cross-section. The output voltage was digitized by an oscilloscope at a rate of 4 giga-samples per second for further offline signal processing. Traces were averaged over 4,096 repeating pump pulses.

Fig. 3 presents a reference trace of the normalized probe wave phase modulation as a function of time, taken on one section of fiber prior to exposure to gamma radiation. The three panels show different time scales. A first and strongest impulse at time $t = 0$ is due to the cross-phase modulation of the probe by the pump pulse through the Kerr effect. A primary series of
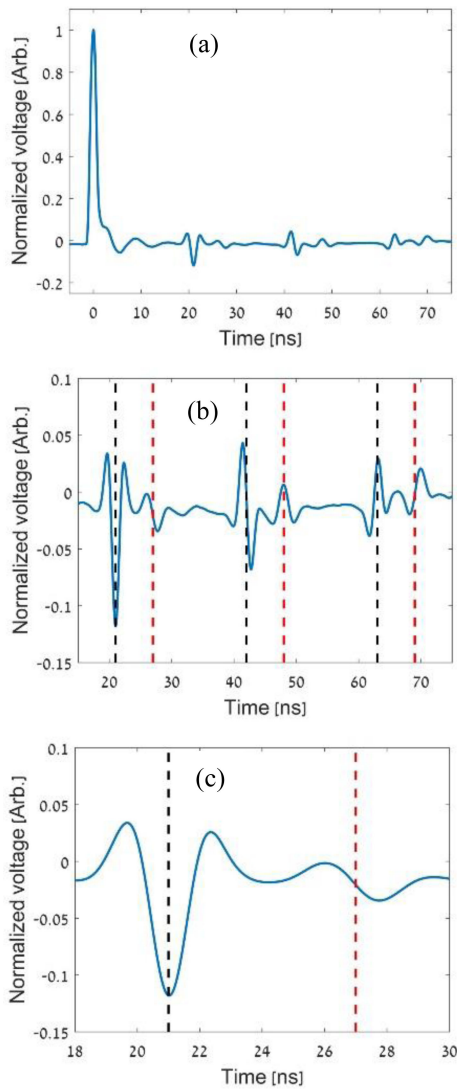
Fig. 3. Measured normalized phase modulation of the output probe wave as a function of time, on a reference fiber section prior to radiation exposure. The three panels show different time scales. A first impulse at time $t = 0$ represents cross-phase modulation by the pump pulses through Kerr nonlinearity. A primary series of events (vertical dashed black lines) is due to photo-elastic modulation by successive echoes of the acoustic wave packet, following multiple reflections from the boundary between coating and cladding. A secondary series of impulses corresponds to reflections at the outer coating boundary (vertical dashed red lines). The time difference between adjacent primary and secondary events represents the two-way time-of-flight of dilatational acoustic waves through the coating layer.

events (black dashed lines) at fixed intervals of 21 ns represents photo-elastic modulation of the probe due to successive reflections of the acoustic wave packet at the boundary between cladding and coating. This time difference equals the two-way acoustic propagation delay from the fiber axis to the edge of the silica cladding and back [52]. The duration of impulses is on the order of 1.5 ns, corresponding to the duration of pump pulses and the acoustic propagation time across the fiber's mode field diameter. A secondary series of impulses (red dashed lines) stems from reflections of the acoustic wave packet at the coating outer boundary. Successive echoes take up different temporal

shapes since the frequencies of acoustic modes are not integer multiples of a unit value [44], [45], [52].

Data analysis focuses on the time difference between a pair of adjacent primary and secondary reflections (see Fig. 3). This difference of 6.0 ± 0.03 ns denotes the two-way time-of-flight of dilatational acoustic waves across the coating layer. We arbitrarily mark the first primary event at the minimum dip and the corresponding secondary event at the maximum slope (Fig. 3). That choice assists in subsequent correlation processing (see below), but it is not unique: other features may be used to identify changes in times-of-flight as long as the choice remains consistent for all samples.

The two-way acoustic time-of-flight through this fluoroacrylate coating layer was previously found to increase by 43 ps per °K [52]. Temperature in the standard, air-conditioned characterization laboratory varied by ± 2 °C among experiments performed over several months. The fibers under test were coiled over few-centimeters radius, and placed on the optical table of the laboratory. The temperatures of the fiber samples were uniform along their lengths during data acquisition. Temperature was measured during each acquisition using a standard laboratory thermometer, placed next to the coiled fibers. The uncertainty in the temperature measurements was ± 0.1 °C. All observed times-of-flight were corrected to a common reference temperature of 22 °C.

Fig. 4(a) shows a magnified view of the normalized output probe phase modulation for several fiber sections following different radiation doses between 50 and 180 Mrad. The reference trace of Fig. 3 is drawn again for comparison. The first primary reflections of all traces were aligned at $t = 21$ ns. Radiation-induced changes to the acoustic time-of-flight across the coating were identified through cross-correlation between the secondary impulse in a fiber under test and the corresponding event in the reference trace. The acoustic time-of-flight across the coating layer is seen to decrease monotonically with the overall dose of gamma radiation between 17 and 180 Mrad (Fig. 4(b)). The change $\Delta\tau$ reached 900 ps, or 15% of the reference value, for the largest dose tested.

The time-of-flight measurement uncertainty $\pm\sigma_\tau$ was estimated as ± 30 ps, or $\pm 0.5\%$ of the mean value, based on the standard deviation of five measurements of each sample taken at one-week intervals following irradiation. The repeating measurements (not shown) did not reveal any annealing or recovery trends of the acoustic times-of-flight, which remained stable. Linear regression of the experimental data yielded a best-fitted slope S of -5.3 ps $\times$ Mrad^{-1} (Fig. 4(b)), with 95% confidence intervals $\pm\sigma_S$ of ± 0.6 ps $\times$ Mrad^{-1}. The radiation dose absorbed by a given sample can be estimated as $D = \Delta\tau/S$, with an experimental error $\pm \sigma_D = \pm\sqrt{2\sigma_\tau^2 + (\sigma_S D)^2}/S$. The uncertainty is $\pm\sqrt{2}\sigma_\tau/S \approx \pm 8$ Mrad for low radiation doses and approaches $\pm(\sigma_S/S)D \approx \pm 0.11D$ for large values.

The transmission losses of the fiber samples were measured during each opto-mechanical experiment: five times over the course of five weeks following irradiation. The mean losses varied between 1-2 dB, and the standard deviations among the five measurements of each sample were between ± 0.5 dB and ± 1
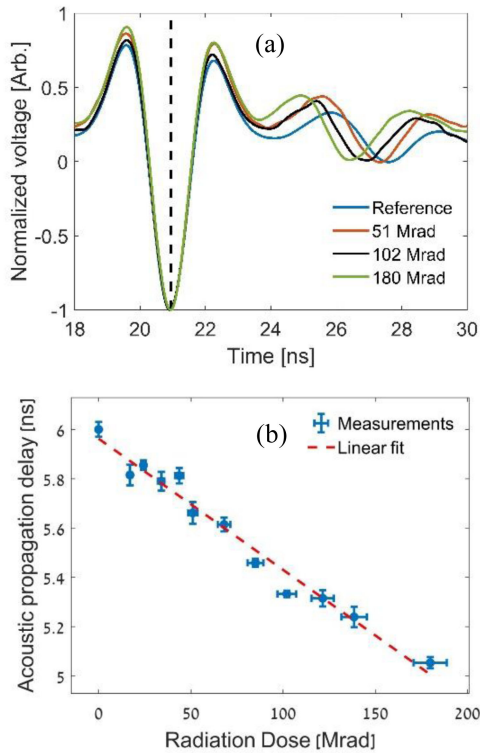
Fig. 4. (a) Measured normalized phase modulation of the output probe wave as a function of time, for several fiber sections following different doses of gamma radiation from a cobalt source (see legend). The timing of a primary acoustic reflection event from the boundary between cladding and coating is noted by a vertical dashed black line, as in Fig. 3 before. The two-way acoustic time-of-flight across the coating decreases with the radiation dosage. (b) Measured two-way acoustic time-of-flight across the coating layer as a function of the overall dose of gamma radiation (blue circular markers). The dashed red line shows best-fitted linear regression.

dB. The mean losses and experimental uncertainty are primarily due to splices and connectors. The uncertainty in transmission losses over the short fiber sections under test corresponds to tens of dB per km [24], [57]. We could not identify a trend of increased attenuation as a function of radiation dose, due to the short fiber lengths. We did not observe trends of changes in transmission losses over time since the end of exposure either. Losses were measured days and weeks after the end of radiation exposure, so transmission may have recovered.

Mechanical measurements of fiber samples were performed off-line. Samples were mounted in a PI85 pico-indenter (Hysitron Incorporated), equipped with a Berkovich indenter probe. The entire pico-indenter load frame was installed in an Ultra Pus scanning electron microscope (Zeiss) to visualize and record the experiments. The samples were positioned to be perpendicular to the indenter probe. The indentation cycle included transverse force load at a constant rate of $200 \, \mu N \times s^{-1}$, a constant loading force of $5,000 \, \mu N$ for 40 seconds, and force unload at the same constant rate. The displacement of the tip inside the coating layer was continuously recorded with a resolution of 0.02 nm. The stiffness of the coating layer was calculated from the measured curves of displacement *vs.* load [53], [54].

The stiffness of the coating layer increased from 30.0 ± 1.8 $\mu N \times nm^{-1}$ in a reference sample to $35.5 \pm 2.4 \, \mu N \times nm^{-1}$ following 102 Mrad dose of gamma radiation. Although this difference is only slightly larger than the measurement uncertainties, the trend of stiffness increase is consistent with faster acoustic velocity following exposure. The measured stiffness subject to static and plastic deformation of the coating layer cannot be directly and quantitatively related to the velocities of high-frequency, elastic acoustic waves. Nevertheless, radiation-induced changes to the layer properties could be qualitatively identified.

Fourier transform infrared (FTIR) spectroscopy analysis of the coatings was carried out using a Thermo Fisher iS50 spectrometer in attenuated total reflection configuration [37]. A germanium internal reflection element was utilized. The infrared beam probed about 1 μm depth of the analyzed coating layer [58]. The measurements did not reveal measurable differences between the reference and samples exposed to 34, 85 and 102 Mrad of gamma radiation. This observation is in agreement with a previous study [37].

The tensile strengths of two fiber samples were measured using two-point bending (Fiber Sigma Instruments) at a strain rate of 4% per minute. The measurements evaluate the strength of the silica fiber within a short equivalent length of 20-200 μm near the bending tip [59]. The fibers were pre-conditioned at 23 $\pm 2 \, °C$ and $50 \pm 5\%$ relative humidity for at least 12 hours before strength testing. The mechanical strengths of the reference fiber section and the sample irradiated by 102 Mrad were found to be 5.3 and 5.7 GPa, respectively. The two measurements are insufficient for drawing conclusions regarding the strengths of irradiated samples. However, the absence of the strength degradation is consistent with handling and visual inspection, which did not reveal qualitative deterioration of the fiber itself or the coating layer.

III. Discussion

Effects of gamma radiation on mechanical properties of the thin polymer coating layer of a standard fiber were observed using forward stimulated Brillouin scattering analysis. Optical pump pulses launched a packet of guided acoustic waves which propagated radially, outward from the core of the fiber. The acoustic time-of-flight across the coating layer was retrieved through the monitoring of multiple acoustic echoes, reflected from the boundaries between cladding and coating and between coating and air. The time-of-flight in the specific coating of fluoroacrylate polymer decreased monotonically with the overall dose of fixed-rate gamma radiation from a cobalt source. Variations reached 900 ps, or 15% of the initial value, following 180 Mrad dose. Radiation-induced changes remained stable over at least several weeks following exposure. The faster times-of-flight observed are corroborated by a measured increase in the stiffness of the coating layer following exposure.

The quantitative estimate of radiation in real time using the proposed method would require the tracking of temperature with sub-°K accuracy, otherwise the detection may be misinterpreted. Distributed temperature measurements may be performed using

a number of established optical fiber-sensing protocols, such as: distributed Raman scattering analysis [60], OFDR of Rayleigh back-scatter [39]–[42], [61], phase-sensitive optical time domain reflectometry (phi-OTDR) based on the same mechanism [62], or Brillouin optical time-domain analysis (B-OTDA) using backward stimulated Brillouin scattering [7], [8]. The fiber sensor systems would also identify possible changes in temperature due to the radiation itself or due to radiation-inued absorption of light. The application of established fiber sensing protocols alongside our proposed technique could help remove the ambiguity in measurements of temperature and radiation.

In addition, the measurements of acoustic wave packet echoes provide an inherent temperature calibration, since the acoustic time-of-flight through the silica cladding is measured as part of the acquisition protocol. Acoustic velocity in silica decreases by $0.6 \, \mathrm{m} \times \mathrm{s}^{-1}$ per °K [52]. Note that the monitoring of coating layer properties described in this work is separate and independent of optical properties of the fiber itself, such as its refractive index or Brillouin frequency shift. Standard Brillouin sensors, such as B-OTDA, do not address the coating layer. The Brillouin frequency shift and the refractive index of the fiber were not measured as part of this work.

The uncertainty in radiation dose estimates was on the order of ±10% for tens of Mrad exposure or higher. Variations in coating diameter among different fiber sections may have contributed to the measurement error. Adjacent samples from the same fiber reel were used in our experiment, hence coating thickness differences were likely to be small. Specific reference traces can be recorded from each section prior to irradiation, to reduce this potential source of error even further.

The minimum dose initiating a detectable change in opto-mechanical properties was on the order of 10 Mrad. To put this level in perspective, a similar overall dose of gamma radiation is accumulated within the core of a few-MW nuclear reactor within minutes (although the energies spectrum is not the same as that of a cobalt source). This dose is also similar to those of typical sterilization equipment. The minimum detectable radiation dose is comparable with that of attenuation measurements at 1,550 nm wavelength over standard single-mode fibers of similar lengths (10 meters) [24]. Specialty fiber coatings may be developed for higher radiation sensitivity, with no modifications required to the fiber itself.

The signal-to-noise ratio (SNR) of the collected traces scales with the fiber length. For the 6–10 meters lengths used, the accuracy of acoustic delay measurements is restricted by the limited bandwidth of forward Brillouin scattering in SMF, several hundreds of MHz, and not by the SNR. The length of fibers used in opto-mechanical analysis has been successfully reduced below 1 meter [63]. The measurement of times-of-flight over shorter sections may be limited by poor SNR.

Radiation effects on acoustic times-of-flight may also indicate variations in the polymer layer density, chemical modifications, or changes at the interface between cladding and coating [39]–[42]. The observation may be compared with previous reports of radiation effects on coated fibers, such as in OFDR calibration [39]–[42]. Protocols for the pre-treatment of the coated fibers, developed towards OFDR [39]–[42], may be applicable to the

detection of radiation as well. Heating of the fibers during radiation exposure does not exceed a few degrees Kelvin [64], and it would not lead to permanent thermal changes in the coating layer.

The maximum radiation exposure could be limited by coating degradation. Radiation effects on the specific polymer will be examined further in future work. The exposure of the fiber can be restricted by excessive radiation induced optical losses as well [24]. The characterization of radiation induced losses requires longer fiber sections. Above a certain limit of radiation exposure, sensing fibers would have to be eventually replaced.

Over the last three years, our group and others reported several protocols for the spatially distributed analysis of forward Brillouin scattering along optical fibers [46]–[49]. The spatial resolution of the analysis has been recently brought to below 1 meter [48], [49]. Other protocols reached kilometers range [46], [47]. This research subject benefits from rapid and exciting progress. These protocols are directly applicable to the spatially distributed forward Brillouin scattering-based mapping of elastic properties of the coating layer [50]–[52]. The technique is suitable for continuous monitoring of fibers protected within cables.

Similar to other measurement protocols, we anticipate that the opto-mechanical response of a fiber would depend on the overall dose, rate, type and energy of ionizing radiation, and vary with the specifics of the coating layer and external conditions. In particular, quantitative interpretation of data might be challenging due to ambiguity between rate and dose. However, the application of opto-mechanical sensing in conjunction with established fiber-optic methods might help disambiguate the monitoring of multiple radiation metrics.

IV. Conclusion

Fiber-optic monitoring of ionizing radiation is drawing great interest and represents a complex challenge. The results presented in this study may serve as a basis for a new detection and sensing concept. Unlike most known techniques, measurements track elastic, rather than optical, observable quantities and address the coating layer and not the silica fiber itself. The extension of the proposed approach towards quantitative dosimetry requires much further work. Nevertheless, opto-mechanical analysis may add a new dimension to fiber-optic sensing of ionizing radiation.

References

[1] Y. Sanada, T. Sugita, Y. Nishizawa, A. Kondo, and T, Torii, "The aerial radiation monitoring in japan after the fukushima daiichi nuclear power plant accident," *Prog. Nucl. Sci. Technol.*, vol. 4, no. 7, pp. 76–80, 2014.

[2] K. R. Kase, Ed. *The Dosimetry of Ionizing Radiation*. Orlando FL, USA: Academic Press, 1985.

[3] P. Andreo, D. T. Burns, A. E. Nahum, J. Seuntjens, and F. H. Attix, *Fundamentals of Ionizing Radiation Dosimetry*. Weinheim, Germany: Wiley, 2017.

[4] E. Udd and W. B. Spillman, Eds. *Fiber Optic Sensors: An Introduction For Engineers and Scientists,* 2nd ed., Hoboken NJ, USA: Wiley, 2011.

[5] K. T. V. Grattan and B. T. Meggit, Eds. *Optical Fiber Sensor Technology Volume 4, Chemical and Environmental Sensing.* Dordrecht, the Netherlands: Kluwer Academic Publishers, 2010.

[6] M. K. Barnoski and S. M. Jensen, "Fiber waveguides: A novel technique for investigating attenuation characteristics," *Appl. Opt.*, vol. 15, no. 9, pp. 2112–2115, Sep. 1976.

[7] T. Kurashima, T. Horiguchi, and M. Tateda, "Distributed-temperature sensing using stimulated Brillouin scattering in optical silica fibers," *Opt. Lett.*, vol. 15, no. 18, pp. 1038–1040, Sep. 1990.

[8] M. Niklès, L. Thévenaz, and P. A. Robert, "Simple distributed fiber sensor based on Brillouin gain spectrum analysis," *Opt. Lett.*, vol. 21, no. 10, pp. 758–760, May 1996.

[9] E. J. Friebele, D. L. Griscom, and G. H. Sigel, "Defect centers in a germanium-doped silica core optical fiber," *J. Appl. Phys.*, vol. 45, no. 8, pp. 3424–3428, Aug. 1974.

[10] I. Toccafondo *et al.*, "Distributed optical fiber radiation sensing in a mixed-field radiation environment at CERN," *J. Lightw. Technol.*, vol. 35, no. 16, pp. 3303–3310, Aug. 2017.

[11] D. Di Francesca *et al.*, "Qualification and calibration of single-mode phosphosilicate optical fiber for dosimetry at CERN," *J. Lightw. Technol.*, vol. 37, no. 18, pp. 4643–4649, Sep. 2019.

[12] G. Cheymol, H. Long, J. F. Villard, and B. Brichard, "High level gamma and neutron irradiation of silica optical fibers in CEA OSIRIS nuclear reactor," *IEEE Trans. Nucl. Sci.*, vol. 55, no. 4, pp. 2252–2258, Aug. 2008.

[13] H. Henschel, O. Köhn, and H. U. Schmidt, "Optical fibres as radiation dosimeters," *Nucl. Instrum. Methods Phys. Res. B*, vol. 69, no. 2/3, pp. 307–314, Jun. 1992.

[14] A. L. Tomashuk, M. V. Grekov, S. A. Vasiliev, and V. V. Svetukhin, "Fiber-optic dosimeter based on radiation-induced attenuation in P-doped fiber: Suppression of post-irradiation fading by using two working wavelengths in visible range," *Opt. Exp.*, vol. 22, no. 14, pp. 16778–16783, Jul. 2014.

[15] S. Girard *et al.*, "Radiation effects on silica-based optical fibers: Recent advances and future challenges," *IEEE Trans. Nucl. Sci.*, vol. 60, no. 3, pp. 2015–2036, Jun. 2013.

[16] S. Girard *et al.*, "Recent advances in radiation-hardened fiber-based technologies for space applications," *J. Opt.*, vol. 20, no. 9, Aug. 2018, Art. no. 093001.

[17] A. Faustov *et al.*, "Highly radiation sensitive type IA FBGs for future dosimetry applications," *IEEE Trans. Nucl. Sci.*, vol. 59, no. 4, pp. 1180–1185, Aug. 2012.

[18] F. Berghmans and A. Gusarov, "Fiber Bragg grating sensors in space and nuclear environments," in *Fiber Bragg Gratings Sensors: Thirty Years from Research to Market*, A. Cusano, A. Cutolo, and J. Albert, Eds. Sharjah, United Arab Emirates: Bentham Science, 2011, pp. 218–237.

[19] K. Krebber, H. Henschel, and U. Weinand, "Fibre Bragg gratings as high dose radiation sensors?" *Meas. Sci. Technol.*, vol. 17, no. 5, pp. 1095–1102, Apr. 2006.

[20] A. L. Huston, B. L. Justus, P. L. Falkenstein, R. W. Miller, H. Ning, and R. Altemus, "Remote optical fiber dosimetry," *Nucl. Instrum. Methods Phys. Res. B*, vol. 184, no. 1-2, pp. 55–67, Sep. 2001.

[21] D. Sporea, A. Sporea, S. O'Keeffe, D. McCarthy, and E. Lewis, "Optical fibers and optical fiber sensors used in radiation monitoring," in *Selected Topics on Optical Fiber Technology*, M. Yasin, S. W. Harun, and H. Arof, Eds., London, UK: Intech Open, 2012.

[22] E. Regnier, I. Flammer, S. Girard, F. Gooijer, F. Achten, and G. Kuyt, "Low-dose radiation-induced attenuation at infrared wavelengths for P-doped, Ge-doped and pure silica-core optical fibres," *IEEE Trans. Nucl. Sci.*, vol. 54, no. 4, pp. 1115–1119, Aug. 2007.

[23] S. Girard *et al.*, "Radiation effects on silica-based preforms and optical fibers - I: Experimental study with canonical samples," *IEEE Trans. Nucl. Sci.*, vol. 55, no. 6, pp. 3473–3482, Dec. 2008.

[24] A. V. Faustov *et al.*, "Comparison of gamma-radiation induced attenuation in al-doped, P-Doped and ge-doped fibres for dosimetry," *IEEE Trans. Nucl. Sci.*, vol. 60, no. 4, pp. 2511–2517, Aug. 2013.

[25] M. Govindarajan and W. Windl, "Atomic-scale modeling of the effects of irradiation on the optical properties of silica glass fibers," *Trans. Amer. Nucl. Soc.*, vol. 104, no. 1, pp. 33–34, Jun. 2011.

[26] A. I. Gusarov and S. K. Hoeffgen, "Radiation effects of fiber gratings," *IEEE Trans. Nucl. Sci.*, vol. 60, no. 3, pp. 2037–2053, Jun. 2013.

[27] P. Niay *et al.*, "Behaviour of Bragg gratings, written in germanosilicate fibers, against γ-ray exposure at low dose rate," *IEEE Photon. Technol. Lett.*, vol. 6, no. 11, pp. 1350–1352, Nov. 1994.

[28] H. Henschel, S. K. Hoeffgen, K. Krebber, J. Kuhnhenn, and U. Weinand, "Influence of fiber composition and grating fabrication on the radiation sensitivity of fiber Bragg gratings," in *Proc. IEEE, 9th Eur. Conf. Radiat. Effects Compon. Syst.*, 2007, pp. 1–8.

[29] S. Girard *et al.*, "Overview of radiation induced point defects in silica-based optical fibers," *Rev. Phys.*, vol. 4, Apr. 2019, Art. no. 100 032.

[30] H. Henschel, D. Grobnic, S. K. Hoeffgen, J. Kuhnhenn, S. J. Mihailov, and U. Weinand, "Development of highly radiation resistant fiber Bragg gratings," *IEEE Trans. Nucl. Sci.*, vol. 58, no. 4, pp. 2103–2110, Aug. 2011.

[31] A. Morana *et al.*, "Radiation tolerant fiber Bragg gratings for high temperature monitoring at MGy dose levels," *Opt. Lett.*, vol. 39, no. 18, pp. 5313–5316, Sep. 2014.

[32] G. L. Vecchi *et al.*, "Infrared radiation induced attenuation of radiation sensitive optical fibers: Influence of temperature and modal propagation," *Opt. Fiber Technol.*, vol. 55, Feb. 2020, Art. no. 102166.

[33] D. Alasia, A. Fernandez Fernandez, L. Abrardi, B. Brichard, and L. Thévenaz, "The effects of gamma-radiation on the properties of Brillouin scattering in standard Ge-doped optical fibres," *Meas. Sci. Technol.*, vol. 17, no. 5, pp. 1091–1094, Apr. 2006.

[34] X. Phéron *et al.*, "High γ-ray dose radiation effects on the performances of Brillouin scattering based optical fiber sensors," *Opt. Exp.*, vol. 20, no. 24, pp. 26978–26985, Nov. 2012.

[35] A. Morana *et al.*, "Steady-state radiation-induced effects on the performances of BOTDA and BOTDR optical fiber sensors," *IEEE Trans. Nucl. Sci.*, vol. 65, no. 1, pp. 111–118, Jan. 2018.

[36] W. Primak, "Fast-neutron-induced changes in quartz and vitreous silica," *Phys. Rev. B*, vol. 110, no. 6, pp. 1240–1254, Jun. 1958.

[37] A. A. Stolov, B. E. Slyman, D. T. Burgess, A. S. Hokansson, J. Li, and R. S. Allen, "Effects of sterilization methods on key properties of specialty optical fibers used in medical devices," *Proc. SPIE Opt. Fibers Sensors for Med. Diagnostics Treat. Appl. XIII*, 857606, Mar. 2013, vol. 8576.

[38] A. A. Stolov *et al.*, "Effects of sterilization on optical and mechanical reliability of specialty optical fibers and terminations," *Proc. SPIE Opt. Fibers Sensors for Med. Diagnostics Treat. Appl. XIV*, 893806, Feb. 2014, vol. 8938.

[39] S. Rizzolo *et al.*, "Radiation hardened optical frequency domain reflectometry distributed temperature fiber-based sensors," *IEEE Trans. Nucl. Sci.*, vol. 62, no. 6, pp. 2988–2994, Dec. 2015.

[40] S. Rizzolo *et al.*, "Investigation of coating impact on OFDR optical remote fiber-based sensors performances for their integration in high temperature and radiation environments," *J. Lightw. Technol.*, vol. 34, no. 19, pp. 4460–4465, Oct. 2016.

[41] S. Rizzolo *et al.*, "Radiation characterization of optical frequency domain reflectometry fiber-based distributed sensors," *IEEE Trans. Nucl. Sci.*, vol. 63, no. 3, pp. 1688–1693, Jun. 2016.

[42] S. Rizzolo *et al.*, "Evaluation of distributed OFDR-based sensing performance in mixed neutron/gamma radiation environments," *IEEE Trans. Nucl. Sci.*, vol. 64, no. 1, pp. 61–67, Jan. 2017.

[43] G. Mélin *et al.*, "Radiation resistant single-mode fiber with different coatings for sensing in high dose environments," *IEEE Trans. Nucl. Sci.*, vol. 66, no. 7, pp. 1657–1662, Jul. 2019.

[44] Y. Antman, A. Clain, Y. London, and A. Zadok, "Optomechanical sensing of liquids outside standard fibers using forward stimulated Brillouin scattering," *Optica*, vol. 3, no. 5, pp. 510–516, May 2016.

[45] R. M. Shelby, M. D. Levenson, and P. W. Bayer, "Guided acoustic-wave Brillouin scattering," *Phys. Rev. B*, vol. 31, no. 8, pp. 5244–5252, Apr. 1985.

[46] G. Bashan, H. H. Diamandi, Y. London, E. Preter, and A. Zadok, "Optomechanical time-domain reflectometry," *Nature Commun.,* vol. 9, Jul. 2018. Art. no. 2991.

[47] D. Chow, Z. Yang, M. A. Soto, and L. Thévenaz, "Distributed forward Brillouin sensor based on local light phase recovery," *Nature Commun*, vol. 9, Jul. 2018. Art. no. 2990.

[48] C. Pang *et al.*, "Opto-mechanical time-domain analysis based on coherent forward stimulated Brillouin scattering probing," *Optica*, vol. 7, no. 2, pp. 176–184, Feb. 2020.

[49] S. Zaslawski, Z. Yang, and L. Thévenaz, "Distributed optomechanical fiber sensing based on serrodyne analysis," *Optica*, vol. 8, no. 3, pp. 388–395, Mar. 2021.

[50] D. M. Chow and L. Thévenaz, "Forward Brillouin scattering acoustic impedance sensor using thin polyimide-coated fiber," *Opt. Lett.*, vol. 43, no. 21, pp. 5467–5470, Nov. 2018.

[51] H. H. Diamandi, Y. London, G. Bashan, and A. Zadok, "Distributed opto-mechanical analysis of liquids outside standard fibers coated with polyimide," *Appl. Phys. Lett.Photon.*, vol. 4, no. 1, Jan. 2019. Art. no. 016105.

[52] H. Diamandi, Y. London, G. Bashan, K. Shemer, and A. Zadok, "Forward stimulated Brillouin scattering analysis of optical fibers coatings," *J. Lightw. Technol.*, vol. 39, no. 6, pp. 1800–1807, Mar. 2021.

[53] B. J. Briscoe, L. Fiori, and E. Pelillo, "Nano-indentation of polymeric surfaces," *J. Phys. D: Appl. Phys.*, vol. 31, pp. 2395–2405, 1998.

[54] K. A. Rzepiejewska-Malyska *et al.*, "In situ mechanical observations during nanoindentation inside a high-resolution scanning electron microscope," *J. Mater. Res.*, vol. 23, no. 7, pp. 1973–1979, Jul. 2008.

[55] D. A. Simoff, A. A. Stolov, H. Wu, N. E. Reyngold, and X. Sun, "Evolution of fluoropolymer clad fibers," in *Proc. 66th Int. Wire Cable Symp.*, 2017, pp. 29–38.

[56] M. S. Kang, A. Nazarkin, A. Brenn, and P. St. J. Russell, "Tightly trapped acoustic phonons in photonic crystal fibers as highly nonlinear artificial raman oscillators," *Nat. Phys.*, vol. 5, pp. 276–280, Mar. 2009.

[57] G. Berkovic *et al.*, "Characterization of radiation hardened fibers in a research grade nuclear reactor," in *Proc. SPIE Micro-structured Specialty Opt. Fibres VII*, Apr. 2021, vol. 11773 Art. no. 117730V.

[58] A. A. Stolov and D. A. Simoff, "Infrared ATR and reflection microspectroscopy as in-situ characterization techniques for optical fibers and their coatings," in *Infrared Spectroscopy. Theory, Development and Applications*. New York NY, USA: Nova Science Publishers, 2014, pp. 403–468.

[59] M. J. Matthewson, C. R. Kurkjian, and S. T. Gulati, "Strength measurement of optical fibers by bending," *J. Am. Ceram. Soc.*, vol. 69, no. 11, pp. 815–821, Nov. 1986.

[60] G. Bolognini and A. Hartog, "Raman-based fibre sensors: Trends and applications," *Opt. Fiber Technol.*, vol. 19, no. 6, pp. 678–688, Dec. 2013.

[61] J. Song, W. Li, P. Lu, Y. Xu, L. Chen, and X. Bao, "Long-Range high spatial resolution distributed temperature and strain sensing based on optical frequency-domain reflectometry," *IEEE Photon. J.*, vol. 6, no. 3, pp. 1–8, Jun. 2014.

[62] J. Pastor-Graells, H. F. Martins, A. Garcia-Ruiz, S. Martin-Lopez, and M. Gonzalez-Herraez, "Single-shot distributed temperature and strain tracking using direct detection phase-sensitive OTDR with chirped pulses," *Opt. Exp.*, vol. 24, no. 12, pp. 13121–13133, Jun. 2016.

[63] Z. Zheng, Z. Li, X. Fu, L. Wang, and H. Wang, "Multipoint acoustic impedance sensing based on frequency-division multiplexed forward stimulated Brillouin scattering," *Opt. Lett.*, vol. 45, no. 16, pp. 4523–4526, Aug. 2020.

[64] A. Piccolo, S. Delepine-Lesoille, M. Landolt, S. Girard, Y. Ouerdane, and C. Sabatier, "Coupled temperature and γ-radiation effect on silica-based optical fiber strain sensors based on rayleigh and Brillouin scatterings," *Opt. Exp.*, vol. 27, no. 15, pp. 21608–21621, Jul. 2019.

Yosef London received the B.Sc. degree in physics and electrical engineering, and the M.Sc. and Ph.D. degrees in electrical engineering from Bar-Ilan University, Ramat Gan, Israel, in 2013, 2015, and 2020, respectively. He is currently a Postdoctoral Fellow with Soreq NRC, Yavne, Israel.

His research interests include optical fiber sensors, nonlinear optics, and opto-mechanical interactions in fibers and photonic integrated circuits. He was the recipient of the Bar-Ilan University Rector Award for excellence in graduate studies in 2015.

Kavita Sharma received the B.Tech. degree in electronics and communications engineering from Guru Gobind Singh Indraprastha University, New Delhi, India, in 2011, and the M.S. and Ph.D. (dual degree) in electrical engineering from Indian Institute of Technology, Madras, India, in 2018. She is currently a Postdoctoral Fellow with the Faculty of Engineering, Bar-Ilan University, Ramat Gan, Israel.

Her research interests include optical fiber amplifiers and lasers, Q-switched fiber lasers, optical fiber sensors, nonlinear optics, and optomechanical interactions in fibers. She was the recipient of an Exchange Student Travel Grant from the European Union's Seventh Framework Programme, for visiting the University of Southampton, U.K. in 2015. She was also the recipient of the Best Photonics Poster Award in the International Conference on Fiber Optics and Photonics in Delhi, India in 2018.

Hilel Hagai Diamandi received the B.Sc. and M.Sc. degrees in electrical engineering in 2015 and 2017 from Bar-Ilan University, Ramat Gan, Israel, where he is currently working toward the Ph.D. degree in electrical engineering.

His research interests include optical fiber sensors, and opto-mechanical interactions in optical fibers. He was the recipient of the Bar-Ilan University Rector Award for excellence in undergraduate studies twice: in 2013 and 2015, and the same Award for excellence in graduate studies in 2017. In 2018 he was awarded the Azrieli Fellowship for doctoral studies by the Azrieli Foundation.

Mirit Hen received the B.Sc., M.Sc., and Ph.D. degrees in chemistry from Bar-Ilan University, Ramat Gan, Israel, in 2009, 2012, and 2017, respectively. From 2016 to 2018, she was a Postdoctoral Fellow with the Faculty of Engineering, Bar-Ilan University. Since 2018, she has been a Staff Scientist with the same faculty.

Her research interests include surface chemistry, organic chemistry, and fabrication of photonic devices in silicon and glass. She was the recipient of the Academia-Industry Fellowship for the Promotion of Women in Science from the Israeli Ministry of Science, Technology, and Space in 2017.

Gil Bashan received the B.Sc. degree in physics and electrical engineering and the M.Sc. degree in electrical engineering from Bar-Ilan University, Ramat Gan, Israel, in 2016 and 2018, respectively. He is currently working toward the Ph.D. degree in electrical engineering with Bar-Ilan University.

His research interests include optical fiber propagation effects, opto-mechanics, and Brillouin scattering. He was the recipient of the Bar-Ilan University Rector Award for excellence in graduate studies in 2018. In 2020, he was awarded the Adams Fellowship for doctoral studies by the Israel National Academy of Sciences and Humanities.

Elad Zehavi received the B.Sc. degree in 2020 in electrical engineering from Bar-Ilan University, Ramat Gan, Israel (cum laude), where he is currently working toward the M.Sc. degree in electrical engineering.

His research interests include optical fiber propagation effects, opto-mechanics, and Brillouin scattering. He was the recipient of the Dean of Engineering Award for excellence in undergraduate studies in 2017 and 2018.

Shlomi Zilberman received the Ph.D. in physics from Tel Aviv University, Tel Aviv, Israel, in 2013. He is currently a Researcher with Soreq NRC, Yavne, Israel.

His primary interest is in the development of optical fiber sensors for various applications, including structural health monitoring, operation in ionizing radiation environments, and shock wave measurements.

Garry Berkovic received the B.Sc. degree in chemistry from the University of Melbourne, Melbourne, VIC, Australia, and the Ph.D. degree from the Weizmann Institute of Science, Rehovot, Israel. After post-doctoral research with the University of California, Berkeley, Berkeley, CA, USA, he was on the faculty of the Weizmann Institute of Science. Since 1998, he has been with Soreq NRC, Yavne, Israel.

He has authored or coauthored about 140 papers, mainly in the fields of optical-based sensors, nonlinear optics, spectroscopy and advanced materials.

Amnon Zentner received the B.Tech. degree in science and technology teaching in the field of electronics from Tel-Aviv University, Tel Aviv, Israel, in 1986. He has worked as Engineer and Consultant in the electronics and optics industries for more than three decades.

Moshe Mayoni received the B.Sc. degree in electrical engineering from Tel-Aviv University, Tel Aviv, Israel, in 2015. He is currently an Electrical Engineer with Soreq NRC, Yavne, Israel. His work focuses on the effects of radiation on electrical components.

Andrei Aleksandrovich Stolov received the Ph.D. degree in physics in 1985 from Kazan State University, Kazan, Russia, where he became a Senior Research Fellow with the Department of Chemistry. He subsequently held positions as a Visiting Scientist with RUCA University, Antwerp, Belgium, and as a Postdoctoral Fellow with the Polymer Science and Engineering Department, University of Massachusetts, Amherst, Amherst, MA, USA. In 2000, he joined Lucent Technologies (currently OFS) in Avon, CT, as a Member of Technical Staff (since 2017 – Distinguished Member of Technical staff).

He has authored more than 100 publications in the fields of molecular spectroscopy, polymer science, and photonics. His focus with OFS is the development and characterization of polymer coatings for specialty optical fibers.

Olga Kleinerman received the B.Sc. degree in materials engineering and chemistry and the Ph.D. degree in chemical engineering from the Technion, Haifa, Israel in 2007 and 2018, respectively. During 2018–2019, she was a Postdoctoral Fellow with Technion and with the University of Calgary, Calgary, AB, Canada. She is currently a Staff Scientist with the Electron Microscopy Center, Department of Materials Science and Engineering, Technion.

Her research focuses on cryogenic electron microscopy, combined with WAXD, SAXS and neutron scattering.

Ehud Shafir received the B.Sc., M.Sc. and Ph.D. degrees in applied physics and electro-optics from The Hebrew University of Jerusalem, Jerusalem, Israel, the Weizmann Institute of Science, Rehovot, Israel, and Tel-Aviv University, Tel Aviv, Israel, in 1982, 1985, and 1991, respectively. Since 1985, he has been with Soreq NRC, Yavne, Israel.

His main interests encompass optical sensing concepts and architectures, smart structures and structural health monitoring. During his position with Soreq he has spent periods as a Visiting Research Scientist with the Norwegian Institute of Technology, Trondheim, Norway, the Optoelectronics Research Centre in Southampton University, Southampton, U.K., El-Op Electro-Optic Industries, Rehovot, Israel, and the Weizmann Institute of Science, Rehovot, Israel.

Avi Zadok received the Ph.D. degree in electrical engineering from Tel-Aviv University, Tel Aviv, Israel, in 2008. Between 2007 and 2009, he was a Postdoctoral Research Fellow with the Department of Applied Physics, California Institute of Technology, Pasadena, CA, USA. In 2009, he joined the Faculty of Engineering, Bar-Ilan University, Ramat Gan, Israel, where he has been a Full Professor since 2017.

He is the co-author of 160 papers in scientific journals and reviewed proceedings of international conferences. His research interests include fiber-optics, nonlinear optics, integrated photonic devices, and opto-mechanics. He was the recipient of the Krill Award of the Wolf Foundation in 2013. He received a Starter Grant from the European Research Council (ERC) in 2015 and a Consolidator Grant from the same agency in 2020. He was a Member of the Israel Young Academy (2016–2020) and was the Chairman for 2019–2020.